

A global grid model based on “constant area” quadrilaterals

Jan T. Bjørke, John K. Grytten, Morten Hæger,
and Stein Nilsen

Norwegian Defence Research Establishment,
PO Box 115, N-3191 Horten,
jtb@ffi.no or sni@ffi.no

Abstract. The WGS84 ellipsoid is tessellated using quadrilaterals of roughly the same size. The tessellation scheme is developed for the purpose of storing, distributing and analysing global as well as local digital terrain models. Compared with DTED, the new grid has a more uniform distribution of cell sizes. This equal area property of the tiles of the grid is an attractive characteristic in geostatistical and wavelet analysis of the terrain model.

Keywords: Global grid, global tessellation patterns, digital terrain models.

1 Introduction

Partitioning geographical data into cells is a fundamental problem of data processing and storage, because efficient region searches, queries and data storage require that the data space is divided into blocks of manageable size. The blocks can be defined on the basis of different hierarchical or one-level tessellations; for a survey on spatial access methods, see for example Gaede and Günter, [GG98]. For small area applications the tessellation is often carried out in a map projection, but for larger areas the projection errors may be considerable. Therefore, for large areas global partitioning schemes are necessary. There are several approaches to the definition of global tessellations, such as surface tessellation based on triangular or quadrilateral meshes, Kimerling et al., [KSWS99]. Goodchild and Shiren, [GS92], apply a hierarchical triangular mesh, the so called QTM proposed by Dutton, [Dut89]. Another example is the popular Digital Terrain Elevation Data (DTED) format from NIMA, [NIM], which is based on an evenly spaced quadrilateral grid of points. Kimerling et al. [KSWS99] compare different global tessellation methods and conclude that the Icosahedral Snyder Equal-Area (ISEA) projection is the best choice for an equal area partitioning. The ISEA projection tessellates the globe into planar triangles, but since we will apply wavelet transforms on the data, we prefer quadrilaterals. Therefore, the ISEA projection is not well suited for our application.

In several applications of geographical data multiresolution or hierarchical structures provide efficient tools for visualization and analysis. A recursive tessellation of the grid, therefore, is attractive. In a plane, a recursive tessellation is

easy to define, but on the surface of an ellipsoid the cell structure is not obvious. Several strategies for this purpose are proposed in the literature, see for example [Dut89,GS92,KSWS99,Ott01,OH02].

However, since the constant area grid has properties such as: (1) simple definition, (2) equal area, and (3) close relation to the longitude/latitude coordinate system, we decided to develop a global tessellation scheme based on an equal area grid. We call this structure the FFI grid. In our application the equal area quadrilateral is an important property since the grid will be used for terrain modeling based on average interpolating wavelets, [BN01]. The wavelet algorithm can be defined on triangular meshes, but the quadrilateral approach is much simpler to implement.

We have selected the following design criteria:

1. The cells should be quadrilaterals of approximately the same size;
2. The tessellation should provide a hierarchical structure;
3. The topology should be as regular as possible, i.e., a cell should have 4 side and 4 corner neighbours at the same level;
4. The partitioning should support matrix representation of the cells.

When the surface is tessellated into a system of regular rectangular cells so that each cell has four side- and four corner neighbours, the matrix representation can be applied. The matrix data structure is very common in image processing, digital terrain modeling and geographical information systems. The structure considered here has several attractive properties, such as: (1) it is very simple to implement, (2) the regular topology makes neighbour search simple, and (3) the regular metrical size of the cells makes distance calculations simple. Therefore, from a computational point of view the matrix data structure has attractive properties.

2 Grid definition

The FFI grid is a global tessellation of the ellipsoid, based on “constant area” quadrilaterals. Grid cells are almost rectangular with dimension between $1/2 \times 1$ nm (nautical miles) and 1×1 nm. The structure of the grid is similar to the DTED grid, but our definition gives a more uniform cell size. A comparison between DTED and the FFI grid defined here is given at the end of this section.

We start with a coarse partitioning of the ellipsoid, using 30 degree sectors drawn along meridians, and bands, which are areas between two different latitudes. The intersection between a sector and a band is called an i-block (intersection block); see Figure (1).

Each i-block is divided into cells using a regular subdivision. All cells have the same height (one arc minute/nm). The width of a cell is approximately one nautical mile at the lower latitude boundary of each band, and decreases towards the upper latitude boundary.

There are two criteria for determining the height of each band: 1) The width of the cells along the upper boundary should not be smaller than a certain

30 deg. sector

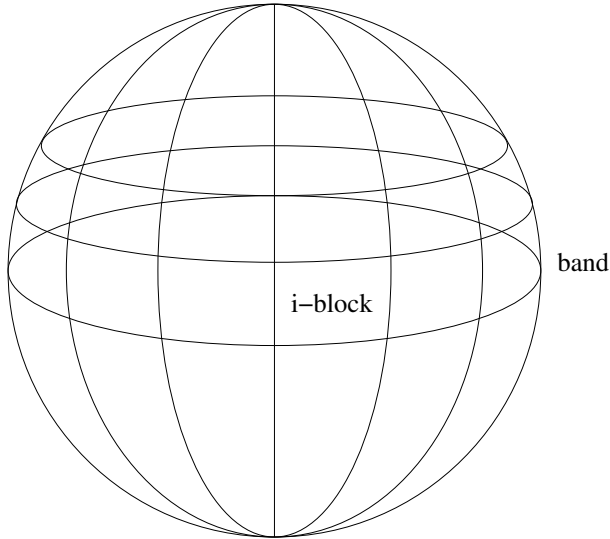


Fig. 1. Definition of bands, sectors and i-blocks

percentage of a nautical mile, and 2) the height of the band, in minutes of latitude, should be divisible by eight.

The latter requirement needs an explanation. In a wavelet representation of a data set, a certain number of cells are needed at the coarsest scale; the exact number is related to the number of taps in the wavelet filters, and will thus depend on which wavelet is used. By using eight by eight cells at the coarsest scale, we have the freedom to choose between several different (average interpolating) wavelets, and can pick the one that best suits the data set.

A collection of eight by eight cells is called an o-block (oct-block). These blocks form a coarse scale representation that can be used, among other things, to navigate the data. There are roughly two million o-blocks on the ellipsoid, which is in the same order of magnitude as the number of pixels on current computer screens.

Exactly how narrow the cells are allowed to become at the upper boundary is shown in the second column of Table (1). The numbers are based on a factorization of the number of minutes in a 30 degree sector. The largest factors (closest to unity) are used for the lower latitudes. As a result of this, no cell between the equator and 75 degrees has an area of less than 80% of an “ideal” 1×1 nm cell. The table also shows the horizontal number of cells within each band, and the exact location of the boundaries between the bands. The factorization column shows that the horizontal number of cells in a 30 degree sector

is divisible by eight for all bands from the equator up to $89^{\circ}52'$, meaning that there are unbroken meridians in the grid for every $3^{\circ}45'$.

We also define sub-cell resolution in the grid by using regular subdivision of each cell. By using a quad-tree representation of the data within each cell, where each node in the tree represents the average value over a sub-cell, we can handle data sets where there are great differences in resolution from area to area. If storage efficiency is an issue, the quad-tree representation can be replaced by an average interpolating wavelet representation, [BN01],[BNar].

Since all cells have roughly the same size and shape, it is easier to construct robust methods for both interpolation and analysis. There is no need to adapt, e.g., variograms to the geometry of the blocks, and coefficients in a wavelet expansion, which can be used to determine gradients or the degree regularity of the data set, have the same interpretation for all cells. For example: the occurrence of large wavelet coefficients indicate sharp gradients in the data. Since all cells have approximately the same size and shape, the steepness of such a gradient will only depend on the level and magnitude of the coefficients, and not on the geographical location of the cell.

bndry #	rel. size	factorization	cells pr. sector	height of band	latitude
0		$2^3 3^2 5^2$	1800(225)	2216(277)	$0^{\circ}00'$
1	4/5	$2^5 3^2 5^1$	1440(180)	680(85)	$36^{\circ}56'$
2	5/6	$2^4 3^1 5^2$	1200(150)	576(72)	$48^{\circ}16'$
3	4/5	$2^6 3^1 5^1$	960(120)	352(44)	$57^{\circ}52'$
4	5/6	$2^5 5^2$	800(100)	328(41)	$63^{\circ}44'$
5	4/5	$2^7 5^1$	640(80)	256(32)	$69^{\circ}12'$
6	4/5	2^9	512(64)	256(32)	$73^{\circ}28'$
7	3/4	$2^7 3^1$	384(48)	248(31)	$77^{\circ}44'$
8	2/3	2^8	256(32)	120(15)	$81^{\circ}52'$
9	3/4	$2^6 3^1$	192(24)	128(16)	$83^{\circ}52'$
10	2/3	2^7	128(16)	120(15)	$86^{\circ}00'$
11	1/2	2^6	64(8)	56(7)	$88^{\circ}00'$
12	1/2	2^5	32(4)	32(4)	$88^{\circ}56'$
13	1/2	2^4	16(2)	16(2)	$89^{\circ}28'$
14	1/2	2^3	8(1)	8(1)	$89^{\circ}44'$
15	1/2	2^2	4	4	$89^{\circ}52'$
16	1/2	2^1	2	2	$89^{\circ}56'$
17	1/2		1	1	$89^{\circ}58'$
18	1/3		1/3	1	$89^{\circ}59'$

Table 1. Relative size of cells across a boundary; number of cells (o-blocks) horizontally within each sector; number of cells (o-blocks) vertically within each band; and location of boundaries between bands.

2.1 Calculation of boundaries between bands

At the equator, the width of a cell is one minute of longitude. As we move towards the poles, the width of the cells decreases, due to the convergence of the meridians. To compensate for this, we introduce bands. Within each band, the vertical cell boundaries follow the same meridians. At the boundaries between the bands, we increase the width of the cells.

To determine where the boundaries between the different bands should be placed, we use the numbers in the first column of Table (1). We start at the equator: the first boundary is placed at the latitude where the radius of the parallel is $4/5$ of the equatorial radius. If we at this latitude increase the size of each cell, so that five cells below the boundary have the same width as four cells above the boundary, the new cells will have the same width as the cells at the equator. The next boundary is placed at the latitude where the radius of the parallel is $5/6 \times 4/5$ of the equatorial radius. Here six cells below the boundary have the same width as five cells above the boundary. Again, the new cells have the same width as the cells at the equator. The same procedure is used to find the rest of the boundaries. The only problem is how to calculate the radius of the parallels at different latitudes.

The reference frame of the grid is WGS 84. This system defines an ellipsoid, which is an oblate spheroid, that can be written on standard form:

$$g(x, y, z) = \frac{x^2}{a^2} + \frac{y^2}{a^2} + \frac{z^2}{b^2} = 1, \quad (1)$$

where a is the equatorial radius, and b is the polar radius. We define the flattening f of the ellipsoid by:

$$f = \frac{a - b}{a}.$$

The parameters for the WGS 84 reference ellipsoid are given by:

$$a = 6\,378\,137\text{ m},$$

$$f = 1/298.257\,223\,563,$$

see, e.g., Hooijberg, [Hoo97].

The latitude ϕ on an ellipsoid is defined as the angle between the normal vector on the surface of the ellipsoid and the horizontal plane, see Figure (2). To find the radius of the corresponding parallel circle, we make use of the following result from differential geometry. A normal vector to the ellipsoid is given by the gradient of g :

$$\mathbf{n} = \nabla g = \left(\frac{\partial g}{\partial x}, \frac{\partial g}{\partial y}, \frac{\partial g}{\partial z} \right) = \left(\frac{2x}{a^2}, \frac{2y}{a^2}, \frac{2z}{b^2} \right). \quad (2)$$

To find the radius of a parallel circle at a given latitude, we only need to consider the part of the surface that lies in the plane $y = 0$. By using Equation

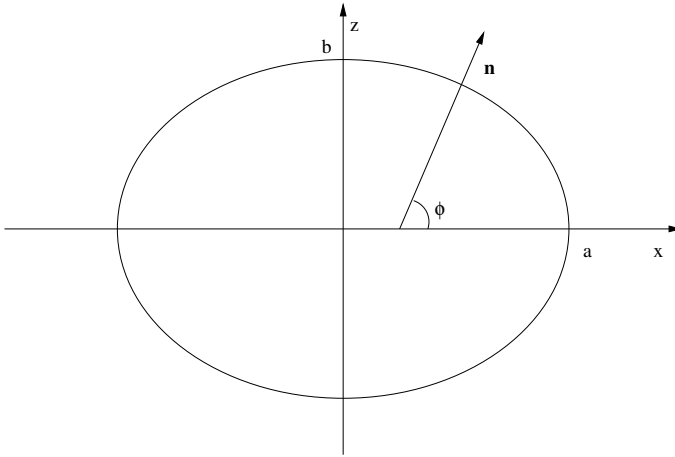


Fig. 2. Section through ellipsoid, definition of latitude angle ϕ

(2) and the definition of f we can express the tangent of the latitude angle in terms of the spatial coordinates:

$$\tan(\phi) = \frac{\partial g}{\partial z} / \frac{\partial g}{\partial x} = (1 - f)^{-2} \frac{z}{x}. \quad (3)$$

By inserting $y = 0$ into Equation (1) we find the equation for the two dimensional ellipse along the zero meridian:

$$x^2 + (1 - f)^{-2} z^2 = a^2. \quad (4)$$

Using Equations (3) and (4) to solve for x , we obtain the following formula for the radius:

$$x = \frac{a \cos(\phi)}{\sqrt{1 + f(f - 2) \sin^2(\phi)}}. \quad (5)$$

This formula gives us the radius of the parallels at different latitudes. We can now search for the latitudes with radii closest to the reduction factors given in Table (1). The only condition is that a boundary should be located at an exact minute of latitude, and that the number of cells within each band should be divisible by eight.

The exact locations of the boundaries are shown in the last column of Table (1). Figures (5) and (6) show the relative widths of the cells in the different bands, and where there are unbroken meridians between bands. Figure (7) shows the grid cells near the pole. How the concepts of cells, o-blocks and i-blocks relate to each other is illustrated in Figure (8).

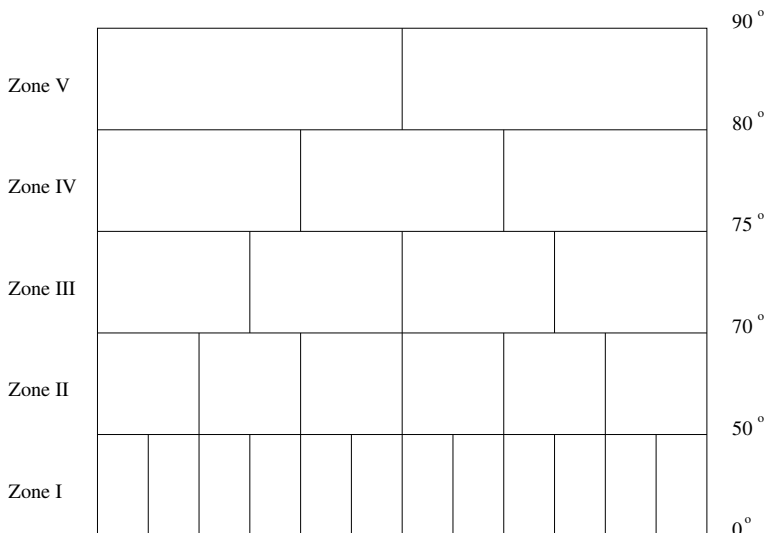


Fig. 3. Illustration of the structure of grid cells in DTED. There are 5 zones in the grid, with zone boundaries at 50, 70, 75 and 80 degrees latitude. For DTED level 1, the horizontal distance between the grid lines, or post spacing, is 3 arc seconds in Zone I, 6 sec. in Zone II, 9 sec. in Zone III, 12 sec. in Zone IV, and 18 sec. in Zone V. The vertical distance between grid lines is 3 sec. in all zones.

2.2 Cell areas compared with DTED

The FFI grid has a structure that is very similar to the structure of the DTED grid. DTED uses five different zones, see Figure (3). For DTED level 1, the width of a cell, or the post spacing, is 3 arc seconds in Zone I, 6 sec. in Zone II, 9 sec. in Zone III, 12 sec. in Zone IV, and 18 sec. in Zone V.

This tessellation has a lot of “half-sized” cells at mid latitudes, and the cells degenerate towards the polar regions.

We have calculated the cell area for all the cells in our grid, as well as for DTED level 1. In order to compare the two grids, we have plotted the results in a relative frequency histogram. Figure (4) shows the relative number of grid cells as a function of cell size. A cell at the equator is defined to have an area of 100%. The width of a class, or box, in the histogram is 5%. Thus, the 80% box shows how many percent of the cells that have areas between 77.5% and 82.5% of an equatorial cell.

We see that all cells in the FFI grid have areas that are 50% or above. Further, more than 90% of the cells have sizes between 82.5% and 102.5%. The distribution of cell sizes for the DTED grid is much wider. We can also clearly see the result of using only one zone, or band, at latitudes above 80 degrees: there are a number of cells with very small area.

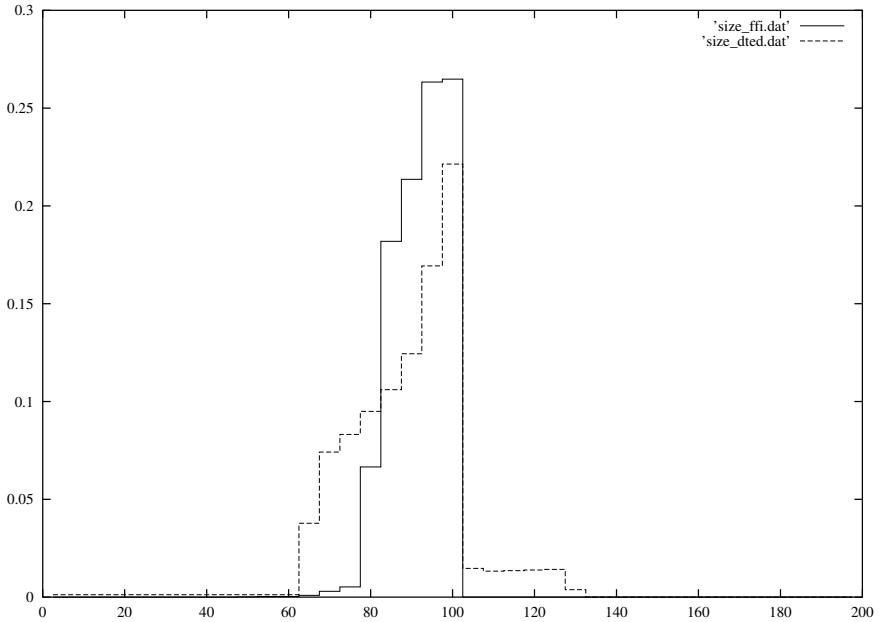


Fig. 4. Relative frequency histogram for distribution of cell areas in DTED level 1, and the FFI grid. Cells at the equator have an area of 100%. Each class in the histogram is 5% wide. The value assigned to each class is the relative number of cells in the grid that have areas that fall within $\pm 2.5\%$ of the center value of the class. We see that the distribution of the FFI grid is more narrow and uniform than DTED.

3 Conclusions

The system of grid cells that we have presented in this paper, called the FFI grid, satisfies our original requirements, i.e., the grid covers the whole globe with cells of approximately the same size, the relationship between the grid and the latitude/longitude system is simple, and the grid system supports a matrix representation. A computation shows that approximately half the cells deviate less than 10% from the normal cell size. Only a small portion of the cells deviate more than 20% from the normal cell size. Compared to the popular DTED grid system the FFI grid is more regular.

The grid cells are well suited as a spatial tiling in a wavelet representation of digital terrain models. A global terrain model represented as wavelet facets, as described here, makes maintenance of the database simple, since the tiling combined with an (average interpolating) wavelet transform makes it possible to split the global model into independent data blocks.

Acknowledgments

This research is supported by the FFI projects SWASI and Viking GIS.

References

- [BN01] Bjørn T. Bruun and Stein Nilsen. Multiscale representation of terrain models using average interpolating wavelets. In J. T. Bjørke and Håvard Tveite, editors, *ScanGIS'2001: Proceedings of the 8th Scandinavian Research Conference on Geographical Information Science*, pages 33–44, Ås, Norway, 25th–27th June 2001.
- [BNar] Bjørn T. Bruun and Stein Nilsen. Wavelet representation of large digital terrain models. *Computers and Geosciences*, to appear.
- [Dut89] G. Dutton. Modeling locational uncertainty via hierarchical tessellation. In M. F. Goodchild and S. Gopal, editors, *Accuracy of Spatial Databases*, pages 125–140. Taylor & Francis, 1989.
- [GG98] Volker Gaede and Oliver Günter. Multidimensional access methods. *ACM Computing Surveys*, 30(2):170–231, 1998.
- [GS92] Michael F. Goodchild and Yang Shiren. A hierarchical spatial data structure for global geographic information systems. *Computer Vision, Graphics and Image Processing: Graphical Models and Image Processing*, 54(1):31–44, 1992.
- [Hoo97] Maarten Hooijberg. *Practical Geodesy using computers*. Springer, 1997.
- [KSWS99] A. Jon Kimerling, Kevin Sahr, Denis White, and Lian Song. Comparing geometrical properties of global grids. *Cartography and Geographic Information Science*, 26(4):271–288, 1999.
- [NIM] NIMA, <http://www.nima.mil/>. *Digital Terrain Elevation Data*. <http://164.214.2.59/srtm/dted.html>.
- [OH02] Patrik Ottoson and Hans Hauska. Ellipsoidal quadtrees for indexing global geographical data. *International Journal of Geographical Information Science*, 16(3):213–226, 2002.
- [Ott01] Patrik Ottoson. Retrieval of geographic data using ellipsoidal quadtrees. In J. T. Bjørke and Håvard Tveite, editors, *ScanGIS'2001: Proceedings of the 8th Scandinavian Research Conference on Geographical Information Science*, pages 89–113, Ås, Norway, 25th–27th June 2001.

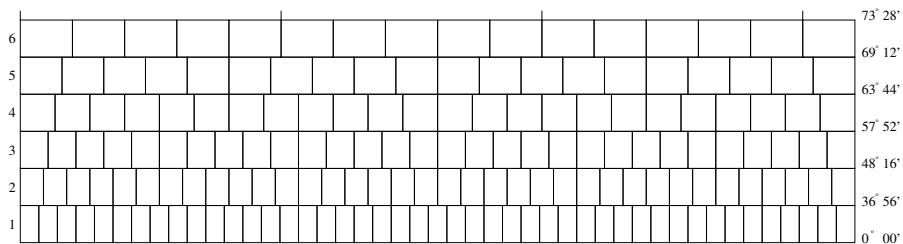


Fig. 5. Structure of the FFI grid: bands from $0^{\circ}00' - 73^{\circ}28'$. All grid cells have the same height of one arc minute. Cells at the equator have a width of one arc minute, but the cell width decreases towards the poles. To compensate for this, bands are introduced. At the boundaries between bands, the width of a cell is approximately one arc minute.

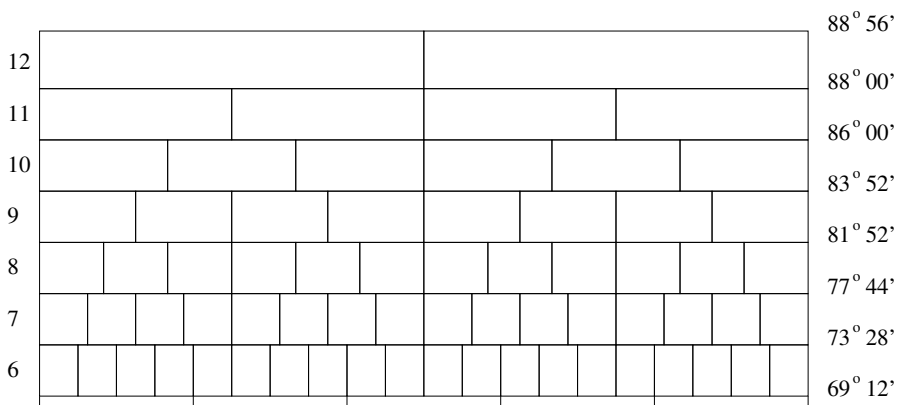


Fig. 6. Structure of the FFI grid: bands from $69^{\circ}12' - 88^{\circ}56'$.

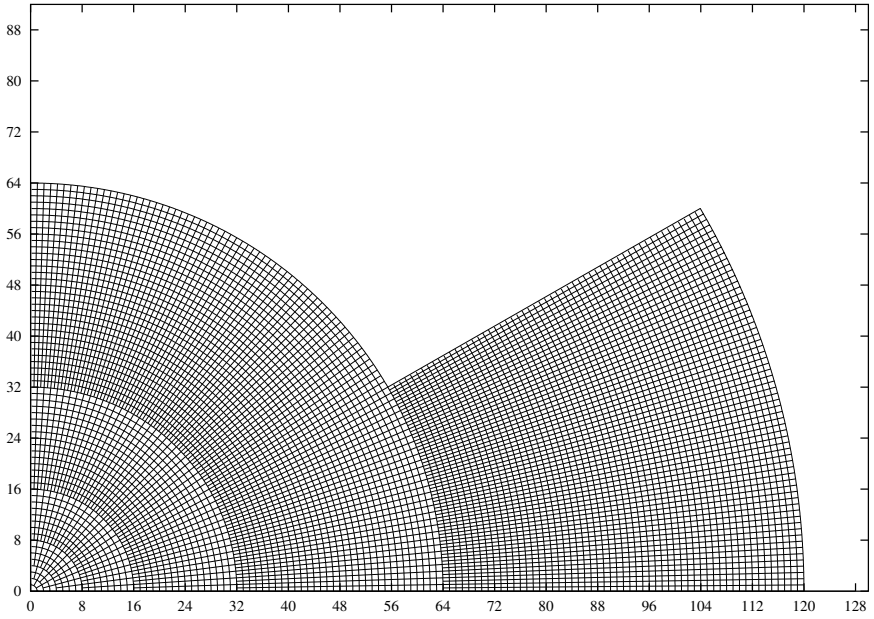


Fig. 7. Cells of the FFI grid from $88^{\circ}00' - 90^{\circ}00'$. The scale on the axes is minutes of arc from the pole.

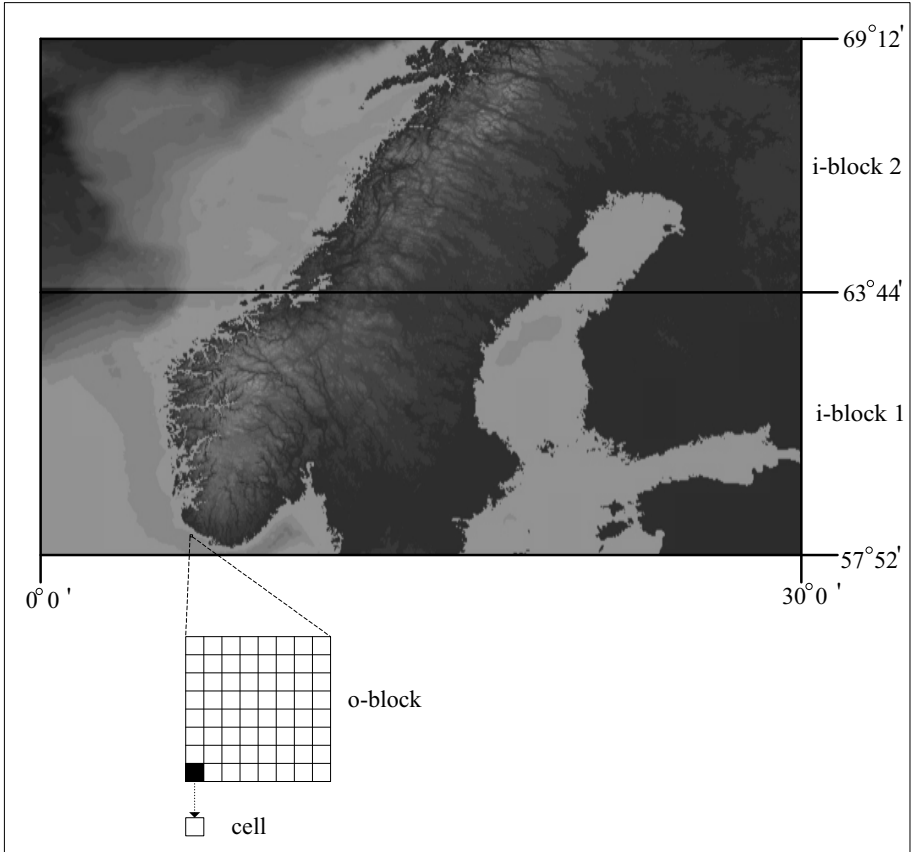


Fig. 8. Demonstration of the size of cells, o-blocks and i-blocks. The cells are of size approximately 1x1 nm. The o-blocks are composed of 8x8 cells, and the i-blocks are intersection areas between the latitude bands and the 30 degree longitude sectors. The figure illustrates two i-blocks.